A Probabilistic Model for the Stress Corrosion Fracture of Glass.

H. Auradou[1)], D. Vandembroucq[2)], C. Guillot[1)] and E. Bouchaud[1)]

1) Commisariat à l'Energie Atomique, Service de Physique et Chimie des Surfaces et Interfaces, Bât. 462, F-91191, Gif-sur-Yvette cedex, FRANCE.
2) Unité Mixte de recherche CNRS/Saint-Gobain "Surface du Verre et Interfaces", 39 quai Lucien Lefranc, F-93303 Aubervilliers cedex, FRANCE

ABSTRACT

The purpose of this paper is to examine the effect of a population of surface flaws on the time to failure of glass under static loading and subject to stress corrosion. The roughness of the glass surface is mapped onto a set of parallel elliptical cracks. The presence of the cracks modified the stress field within the material and induces a shielding of the stress at the cracks tips which increases the lifetime of the material. We show that this effect becomes important when the length of the cracks is comparable to the distance separating them. We also point out that, due to shielding and depending on the crack configuration, others cracks than the longest can lead to the failure of the sample.

INTRODUCTION

An important practical problem is to predict the lifetime of a piece of glass under stress. The failure time depends upon the surface state, the loading and also on the ambient environment. This delayed failure of glass is associated with *the stress-corrosion* growth of pre-existing tiny surface defects in the presence of humidity. The corrosion process has the important consequence that any (sufficient) stress tends to lengthen the flaw and that finally the object breaks after the flaw has reached a critical length. While the fundamental nature of these flaws remains unclear since it is difficult to observe them directly, the presence of surface defects has been clearly highlighted in various experimental conditions [1, 2, 3]. Mechanical contacts or thermal shocks can for example be responsible for surface cracks. However it is well known that freshly drawn fibers can be broken in a stress-corrosion regime while AFM studies could not reveal any flaw on their surface [4]. Later studies [5] showed that the nanometer scale roughness of the fiber surface presented long range correlations (up to 100nm); the surface is in fact self-affine [6], meaning that it is statistically invariant under the transformation $x \rightarrow \lambda x$ and $z \rightarrow \lambda^H z$, where x is a distance in the mean plane of the surface and z a height difference. Here H is the Hurst exponent where $0 < H < 1$. Note that this very gentle roughness is responsible for fluctuations of the tangential stress at the surface, (see Ref.[7] for direct calculations of the stress field from the knowledge of the roughness *via* conformal mapping). In other words even if there is no evidence for flaws on the glass surface, there can be stress concentration effects due to the roughness. We actually propose in this work to map a rough surface onto a set of elliptical cracks distributed over a plane surface so that they are responsible for the same local stress concentrations. Then, we investigate the variations of the time to fracture due to the distribution of cracks. Moreover, we will consider that flaws are microcracks with atomically sharp tips which emerge normally at the external surface of the glass. Thus, we will not consider possible crack blunting [8, 9]. The glass is supposed to be perfectly elastic and submitted to constant remote tension. Due to the presence of neighboring cracks, the stress at the tip of each crack is altered and the cracks do not longer behave as isolated cracks. The following section describes the model used to take into account the cracks interactions in the growing process of the surface flaws.

DESCRIPTION OF THE MODEL

Initial configurations of the cracks : Figure 1 shows the four steps followed to obtain an initial crack configuration.We first start by considering a one dimensional self-affine profile consisting of M facets of size l when projected onto the horizontal plane. We have chosen to generate profiles of Hurst exponent $H = 0.8$ since it is this value that is often found for three-dimensional fractures [6] but others value may be used. The lengths l and $L = Ml$ correspond respectively to the lower and the upper scales of the self-affine description. Furthermore, the average slope, s, of the facets are small enough to allow for the computation by conformal mapping [7] of the local stresses when the profile is considered under uniaxial tension σ_0. Since our interest focuses on the subpart of the profile where the stress is concentrated, parts of the profile where the stress is lower than σ_0 are removed from the computation. We then select from the remaining set of stress the local stress maxima i.e. parts of the profile where the stress is higher than its two nearest remaining stresses. To each of the remaining stresses σ is

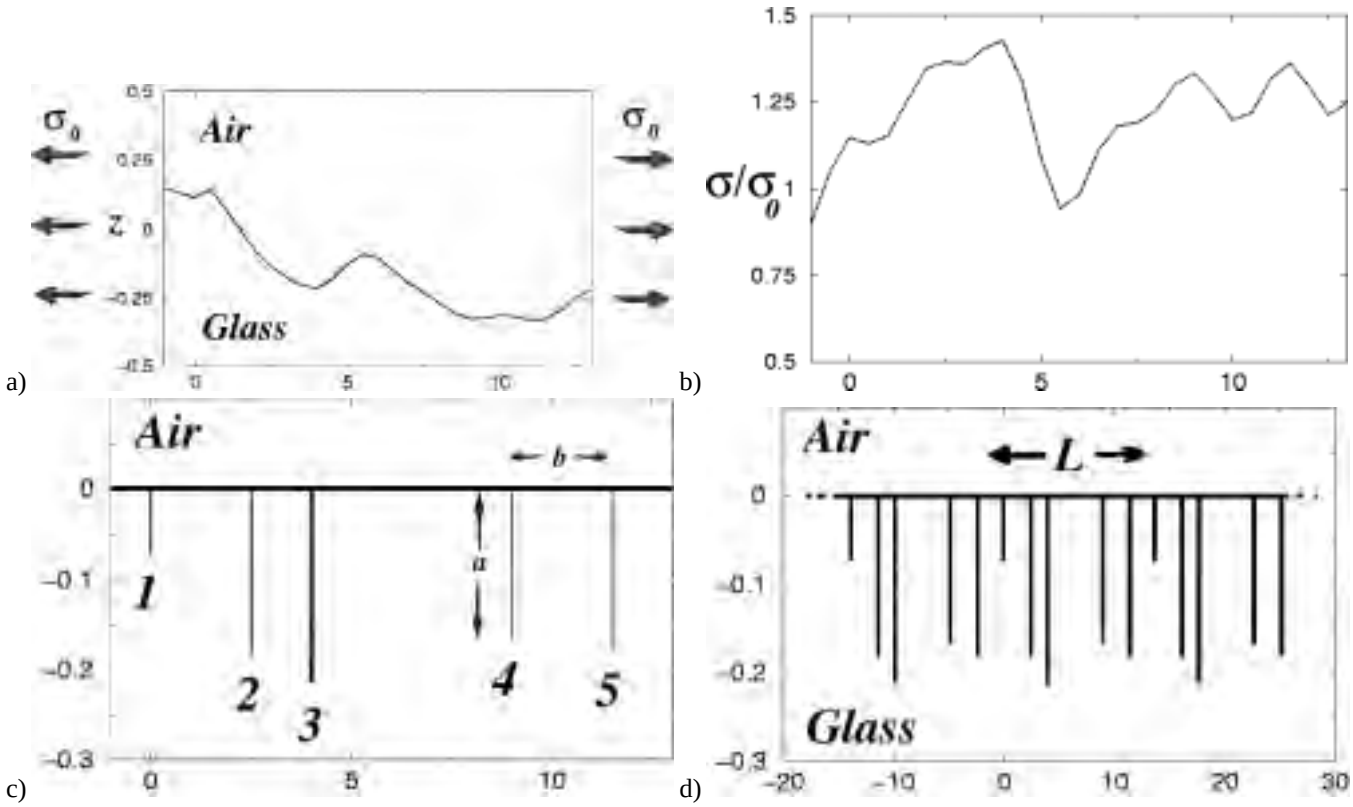

Figure 1: Generation of the initial crack configuration. A smooth self-affine profile with roughness exponent $H = 0.8$ made of M facets of length l and of average slope s (here $M = 15$, $l = 1$ and $s = 0.1$) is first generated (a). The profile is considered under uniaxial tension σ_0. From the height profile, the stress is computed using a conformal mapping technique [7] (b). Parts of the profile where the stress is a local maxima that concentrate the stress *i.e.* $\sigma > \sigma_0$ are selected from the set of stress. A crack of length $a = (\sigma/\sigma_0 - 1)l/2$ is them associated to each place of stress is concentration (c). The figure (d) shows the final crack configuration obtained by translation of the set of cracks. In this example, ratio between the average crack length and the horizontal distance between them is $< a > /b = 0.06$.

associated an equivalent elliptical crack a long by l wide which is under a uniaxial stress σ_0. The length of the hole is chosen so that the stress at the tip of the major axis is the one obtained by the conformal mapping method *i.e.* $\sigma = \sigma_0(1 - 2a/l)$.

The roughness of the profile is thus map onto a set of parallel elliptical cracks that emerge normally to the external surface. The average distance b between the cracks is of the order of few l and the cracks spread over a horizontal distance L. The self-affine profiles generated is made of 20 to 200 facets and the final set of cracks typically contains from 5 to 50 cracks. The set of cracks is then reproduced by translation of constant steps L (*i.e.* periodic boundary conditions); the final crack configurations is thus a succession of identical sub-cracks set that contains cracks of various lengths.

Determination of the Stress Intensity Factors : It is well known that the problem of a linear elastic solid with N cracks can be represented as a superposition of N problems involving one crack but loaded by unknown tractions induced by the other cracks and the remote loading; the so-called *"pseudo-tensions"* [10, 11]. These tractions can be interrelated through a system of integral equations [12]. Recently, a simple and efficient technique to solve this problem based on the superposition technique and the idea of self-consistency applied to the average tractions on individual cracks has been proposed [13, 14].

To introduce this model we will first consider a simple crack configuration which consists of N parallel cracks of same length a and equally space by a distance b embedded in an semi infinite elastic plane. For convenience, the elastic plane is related to a cartesian system of coordinates xOy in such a way that the x and the y axes are respectively normal and along the crack faces. The set of cracks is under a constant remote tension σ_0 applied along the x-direction.

The key assumption of the method is to neglect the stress on the crack i due to the non uniform loading on the other cracks. Thus the traction shed on crack i by the crack j results from the uniform average traction on crack j. In fact, the

impact on crack i of the non-uniformities of the tractions on the crack j is neglected. This result in a major simplification of the problem, self-consitency imposing then to the averaged stresses to be the solution of a simple linear system. Other techniques using a polynomial approximation of the stress non-uniformities were also proposed [15], the method presented here is more efficient in terms of calculation time and was found sufficiently accurate.

According to this simplification, the normal σ_i and the shear τ_i tractions on the crack i can be expressed as a function of the average tranction$< \sigma_j >$and the average shear $< \tau_j >$ on crack j in the following way:

$$\begin{cases} \sigma_i(y) = \sigma_0 + \sum_{j \neq i} \left(\sigma_j^{nn}(y) < \sigma_j > + \sigma_j^{\tau n}(y) < \tau_j > \right) \\ \tau_i(y) = \sum_{j \neq i} \left(\sigma_j^{n\tau}(y) < \sigma_j > + \sigma_j^{\tau\tau}(y) < \tau_j > \right) \end{cases} \tag{1}$$

where $\sigma_j^{nn}(y)$ and $\sigma_j^{n\tau}$ are respectively the remote tension and the shear stress induce on the crack i by the crack j under tension of unit intensity. In the other hand, a shear stress of unit intensity applied on the crack j induces a remote tension $\sigma_j^{\tau n}(y)$ and a shear stress $\sigma_j^{\tau\tau}(y)$ along the crack i. These stresses are expressible in elementary functions [18]. Averaging along the crack i yields, using 1:

$$\begin{cases} < \sigma_i >= \sigma_0 + \sum_{j \neq i} \left(\Lambda_{ji}^{nn} < \sigma_j > + \Lambda_{ji}^{\tau n} < \tau_j > \right) \\ < \tau_i >= \sum_{j \neq i} \left(\Lambda_{ji}^{n\tau} < \sigma_j > + \Lambda_{ji}^{\tau\tau} < \tau_j > \right) \end{cases} \tag{2}$$

where Λ are transmission factors which characterize the transmission of the average stresses acting on the crack j on the crack i. For example, $\Lambda_{ji}^{\tau n}$ is the average normal traction on crack i induced by a uniform shear stress of unit intensity applied on crack j. Equation 2 is valid for any of the cracks; we thus have a system of $2N$ linear algebraic equations for $2N$ unknown average stress. From this set of equation, $< \sigma_i >$ and $< \tau_i >$ can be easily determined for the N cracks.

After $< \sigma_i >$ and $< \tau_i >$ are determined for the N cracks, the tractions on any of the cracks can be determined using 1. The stress intensity factor at the tip of the crack i corresponding to the Mode I, K_I and the Mode II, K_{II} can than be obtained using the following relations [18] :

$$\begin{cases} K_I^i(a) = \frac{1}{\sqrt{\pi a}} \int_0^a \sigma_i(t) \left(\frac{a+t}{a-t} \right)^{1/2} dt. \\ K_{II}^i(a) = \frac{1}{\sqrt{\pi a}} \int_0^a \tau_i(t) \left(\frac{a+t}{a-t} \right)^{1/2} dt. \end{cases}$$

Figure 2 compares results obtained by this method with other works for configurations where all the cracks have the same length. We see that while the ratio between the crack size and the distance between them is small enough, the results are in good agreement with previous works. Yet, discrepancy appears when the cracks length becomes of the order of the distance between them. This discrepancy comes from the fact that the non-uniformities of the tractions are not taken into account in our model. Moreover, it can be shown that the approach used is only valid for $K_I/K_{I0} > 2/3$; this leads to a major restriction on the ratio between the crack length a and the distance between them b which has to be less than unity.

In this work, the crack configurations consist of an infinite number of parallel edge cracks under uniaxial tension applied normal to the crack planes. Even if the cracks do not have the same length the horizontal distance separating them is large enough so that the stress intensity factor, K_I, corresponding to the Mode I loading is always more important than the stress intensity factor, K_{II}, which corresponds to in-plane shear loading. In all the cases presented the ratio K_I/K_{II} is always greater than 100, thus possible crack deflection will not be considered and cracks will open under pure Mode I.

Crack propagation law : From the experimental studies [19, 20, 21, 8], it is clear that crack velocity is strongly affected by the stress assisted corrosion reaction between the glass and the corrosive species in the atmosphere. Moreover, it appears that the velocity is uniquely related to the stress intensity factor. Depending on the stress intensity factor, three different regions are observed. In our work we mainly focus on the so called Region I which corresponds to the low speed regime. In this domain, the speed of the crack typically lies between $10^{-10}$and $10^{-5} m.s^{-1}$. In the other regions, crack propagation is fairly rapid and the range of stress intensity factors involved is narrow. Thus for long enough test times the contribution to the time before rupture in these regions is negligible.

Wiederhorn *et al* [20] carefully studied the low speed domain of the crack growth for various glasses and various environmental conditions. The data were found to fit the equation :

$$v(K_I) = v_0 exp(\frac{-E^* + cK_I}{RT}), \tag{3}$$

where $v(K_I)$ is the crack velocity, T the temperature. $E^*$is the apparent activation energy at zero load and c is the stress intensity factor coefficient. In this work we set the activation energy to zero. This has the consequence that under any applied

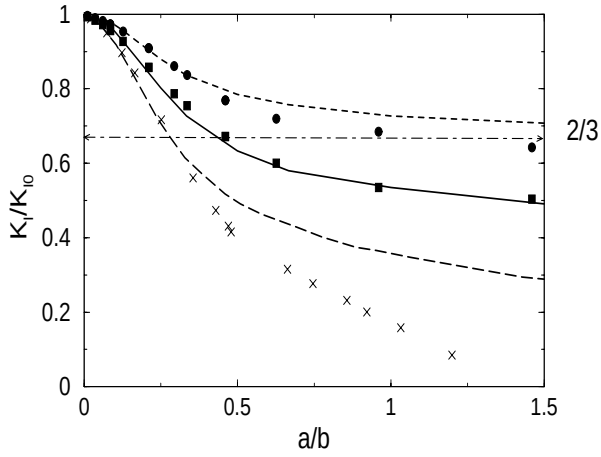

Figure 2: Curves of K_I/K_{I0} vs a/b for a semi infinite elastic plane containing a periodic array of N parallel cracks of same lengths a separated by a constant distance b and subjected to a uniform uniaxial stress σ_0 acting in a direction perpendicular to the cracks. $K_{I0} = 1.12\sigma_0\sqrt{\pi a}$ is the stress intensity factor for an isolated crack $N = 1$. Filled squares and filled circles represent the results obtained in our model for $N = 3$ cracks and correspond respectively to the inner and the outer cracks. The dashed and the solid lines show results from Isida [16]using a body force method for $N = 3$. The crosses show results obtained with our model for an infinite sequence of parallel cracks, these results are compared to the data of Bowie (long dashed line) [17].

stress, all the cracks are allowed to grow independently of their length. By normalizing the speed by the speed v_0 of the cracks at small stress intensity factor, equation 3 becomes :

$$v(K_I) = exp(c^* K_I) \tag{4}$$

with $c^* = c/RT$.

The different steps of the simulation can be summarized as follows :

- computation of the initial crack configuration from a self-affine surface consisting of facets of average slope s and using a conformal mapping technique.
- the stress intensity factor at the tip of each crack is calculated.
- the speed of each of the cracks is obtained using the crack growth law $v(K_I)$.
- the length of each crack is then incremented by $\Delta a = v(K_I)\Delta t$ where Δt is a fixed time step.

The three last steps of the computation are iterated until one of the cracks reaches the critical stress intensity factor K_{Ic} above which failure of the sample occurs. The lifetime of the material is defined as the time need by the crack that reaches K_{Ic} the first to grow from its initial size to its final length. This lifetime will be compared to the lifetime in the absence of stresses shielding. The latter is obtain by considering the longest crack of the initial configuration as isolated and by computing the time needs by this crack to reach K_{Ic}.

QUALITATIVE DESCRIPTION OF THE CRACK GROWTH

We will first start to analyze the results obtained by the model by considering a single cracks configuration.

Figure 3(a) shows the initial cracks configuration at the scale L; we should remind the reader that periodic boundary conditions are applied to our model. In other words, the crack labeled 5 has two next neighbors the crack 4 but also the crack 1. Under the action of the corrosion, the cracks grown until one of them reaches K_{Ic}. Figure 3(b) shows the configuration

just before failure. In this example, the crack interaction have two effects. The first is to increase the lifetime of the sample; here the increase of the lifetime is of the order of 6% compared to the lifetime in the absence of shielding. The interactions lead to an other effect which has to be pointed out : the crack that reaches K_{Ic} the first is not the crack which was initially the longest. In fact, while the longest crack in the initial configuration (fig.3(a)) was the crack labeled 2, the longest crack in the final cracks set (fig.3(b)) is the crack number 5. We also note that the interactions tend to level the length of the cracks. In the beginning of the simulation, the ratio of the length of the longest crack to the average length of the cracks is $a_{max}/ < a >= 2.5$ and when failure occurs the ratio increased to almost 1 (1.003).

The effect of the interactions between the cracks can be highlight by considering the evolution of the ratio between the stress intensity factor for each of the cracks and the stress intensity factor of the cracks when considered as isolated. In figure 4, we see that for small crack size, which correspond to the beginning of the simulation, the ratio of the stress intensity factors is closed to one, meaning that each cracks can be seen as isolated. But while the cracks length increases, this ratio decreases until one of the cracks is long enough so that K_{Ic} is reached and that rupture occurs.

The crack that reaches K_{Ic} the first is the crack 5 which was not the longest crack of the initial configuration. We clearly see on figure 4 that this crack is the one that is less influenced by the interaction. The stress intensity factor associated to this crack is always "roughly" (compares to the others) close to the stress intensity factor in the absence of shielding. Thus is speed is close to the speed that it will have had in the absence of interaction. This is not the case for the crack 2 which is the longest crack of the initial crack configuration. The latter is much more influenced by the shielding of the stress than the crack 5. The fact that its stress intensity factor is less than the one expected in this absence of shielding leads to a crack speed which is less than the speed in absence of shielding. As a consequence, the crack 5 accelerates much faster than the crack 2 and finally the crack 5 overtakes the crack 2.

We see from this example that the presence of a neighborhood of cracks results in a decrease of the stress intensity factors. Due to this shielding effect, the speed of each cracks is lower than what it would have been in the absence of shielding. The progress of the cracks is thus slow down and as a consequence the lifetime of the material increases. The shielding effect will strongly depends on the initial cracks configuration. In the next section, we investigate the effect of the statistical distribution of the crack lengths on the lifetime of the sample.

QUANTITATIVE RESULTS

Depending on the self-affine profile generated, different crack configurations are obtained. These configurations differ in the the crack lengths and also in the arrangement of these cracks and, thus, each configuration will lead to a different lifetime.

Figure 5 shows the distribution of the ratio between the lifetime and the lifetime of the material when the longest crack is considered as isolated. We see that the times ratio are always larger than 1, meaning, as discussed previously, that the interactions between the cracks increase the lifetime of the material. Configurations obtained using $s = 0.1$ give rise to a broad distribution of lifetimes which gets sharp when s decreases.

This effect is mainly due to the change in cracks lengths when the self-affine profile generated gets smoother. In fact, a decrease of the facets slope changes the length of the cracks that shrinks and as a consequence the ratio between the crack length and the distance separating them is decreased. For the configurations studied, the average crack length referred to the distance separating them is $< a > /b = 8.10^{-2}$ when the facets slope s is 0.1, while for $s = 0.01$ this ratio is 8.10^{-3} and drops to 8.10^{-4} when $s = 0.001$. As shown in the previous section, this will deeply influence the shielding effect, that has less influence on the growing process when the ratio $a/b << 1$.

For small $< a > /b$, the cracks grow as if they were isolated, and as a consequence the lifetime of the material is close to the time to failure without shielding. When $< a > /b$ becomes large enough, the shielding effect becomes important and this has a strong effect on the lifetime which can be quite larger than the lifetime without interaction.

CONCLUSION

We have developed a model of crack growth where the modification of the stress field due to the presence of neighboring cracks is taking into account. Our model allow for the computation of the stress intensity factors of sharp cracks under stresses. This model has been applied to stress corrosion growth of pre-existing surface flaws. The initial flaw configuration is obtained by mapping the self-affine roughness of the external surface of the glass considered under tension into a set

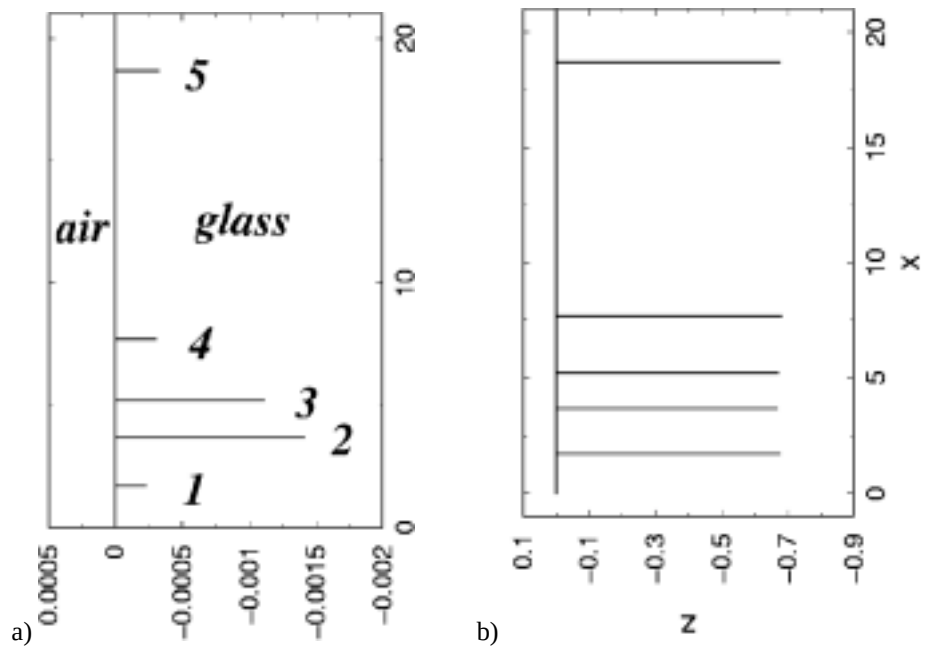

Figure 3: The figure (a) shows the initial crack configuration. consisting of $N = 5$ cracks load by a remote tension $\sigma_0 = 1$. Figure (b) represents the cracks when K_{Ic} is reached. In this simulation the speed of the crack is $v(K_I) = exp(K_I)$ and $K_{Ic} = 1$. Initially the ratio between the average crack length and the distance separating them is $< a > /b = 4.10^{-3}$ and is $< a > /b = 0.28$ when failure occurs.

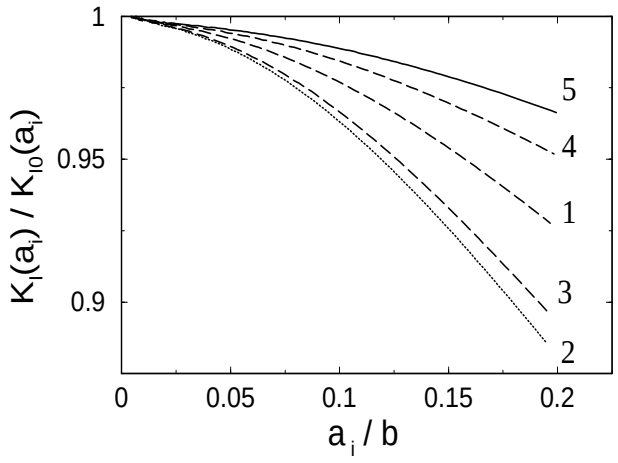

Figure 4: Evolution of the stress intensity factor for the crack configuration shown in Figure 3 as a function of the length a_i of crack i. Here, the relationship between the speed of the crack and the stress intensity factor is : $v(K_I) = exp(K_I)$ and $K_{Ic} = 1$. b is the distance between the cracks. $K_I(a_i)$ is the stress intensity factor of the crack i when cracks interact. $K_{I0}(a_i) = 1.12\sigma_0\sqrt{\pi a_i}$ corresponds to the stress intensity factor of an isolated crack of length a_i .

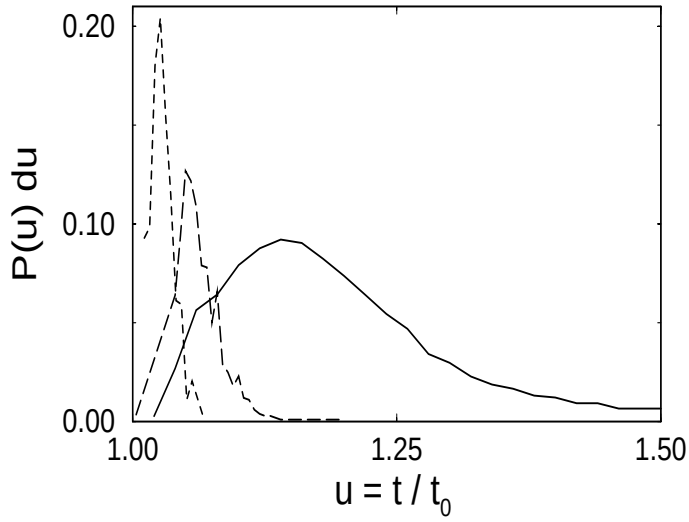

Figure 5: Distribution of the ratio of lifetime, t, when interaction are taking into account to the lifetime, t_0, in the absence of interactions. The data were obtained using 600 initial crack configurations generated using self-affine profiles made of facets of different slopes s. Solid, dotted and long dashed lines correspond respectively to $s = 0.1$, 0.01 and 0.001. The crack velocity law used is $v(K_I) = exp(K_I)$ and $K_{Ic} = 1$.

of parallel elliptical cracks. The growing rate of each crack, that open under pure Mode I, is uniquely related to its stress intensity factors by a relation that fit previous experimental works.

We have shown that the presence of neighboring cracks lead to a shielding of the stresses at the tip of the cracks and to an increase of the time to failure. Moreover this increase of the lifetime becomes non negligible when the shielding effect is important. This is achieved when the crack lengths become of the order of the distance separating them. We have, also, pointed out that, due to shielding and depending on the crack configuration, others cracks than the longest can lead to the failure of the sample.

The effect of the remote tension an the lifetime has been studied also and it appears that the shielding effect has a strong influence on the lifetime when the remote tension is decreased. Further work is presently carried on to characterize the distribution of lifetime in terms of a Weibulh distribution.

References

[1] da C. Andrade, E.N. and Tsien, L.C., "On surface cracks in glass," *Proc. Roy. Soc.* A., 159, 1937, pp. 346-354.

[2] Poloniecki, J.D. and Wilshaw, T.R., "Determination of surface crack size densities in glass," *Nature Physical Science*, 229, 1971, pp. 226-227.

[3] Adams, R. and McMillan, P.W., 'The decoration of surface flaws in glass", *J. Mat. Sci*. 12, 1977, pp. 2544-2546.

[4] Guilloteau, E. (1997), PhD Thesis, University Paris XI, France.

[5] Nghiêm, B. (1998). PhD Thesis, University Paris VI, France.

[6] Feder J., *Fractals*, Plenum press, 1988.

[7] Vandembroucq, D. and Roux, S., "Conformal mapping on rough boundaries. II. Applications to biharmonic problems," *Phys. Rev. E*. 55 [5], 1997, pp. 6186-6196.

[8] Crichton, S.N. and Tomozawa, M., "Subcritical crack growth in a phosphate laser glass," *J. Am. Ceram. Soc* **82** [11], 1999, pp. 3097-3104.

[9] Bando, Y., Ito, S. and Tomozawa, M., "Direct observation of crack tip geometry in SiO_2 glass by high-resolution electron microscopy," *J. Am. Ceram. Soc.* **67** [3], 1984, pp. C36-C37.

[10] Gong S.X. and Horii, H. (1989) *J. Mech. Phys. Solids* **37** (1), 27.

[11] Hori, M. and Hemat-Nasser, S. (1987) *J. Mech. Phys. Solids* **35** (5), 601.

[12] Datsyshin, A.P. and Savruk, M.P., "A system of arbitrarily oriented cracks in elastic solids," *J. Appl. Math. Mech.* **37**, 1973, pp. 306-313.

[13] Kachanov, M., "A simple technique of stress analysis in elastic solids with many cracks," *Int. J. Fracture* **27**, 1985, pp. 113-119.

[14] Kachanov, M. and Montagut, E., "Interaction of a crack with a certain microcrack array," *Eng. Frac. Mech*. 25, 1986, pp. 625-636.

[15] Chudnovsky, A. and Kachanov, M., "Interaction of a crack with a field of micro cracks," *Int. J. Engng. Sci* **21**, 1983, pp. 1009-1018.

[16] Isida, M., "Tension of a half plane containing array of cracks, branched cracks and cracks emanating from a sharp notches," *Trans. Japan Soc. Mech. Engrs.*,**45** [392], 1979, pp. 306-317.

[17] Bowie, O.L. (1972). In:*Method of analysis and solutions of crack problems*, ed. by G.C. Sih, Noordhof Int. Pub. Vol. I.

[18] Sneddon, I.N, and Lowengrub, M, "Crack problems in the classical theory of elasticity" , Wiley New York, 1969.

[19] Wiederhorn, S.M., "Influence of water vapor on crack propagation in Soda-Lime glass," *J. Am. Ceram. Soc* **50** [8], 1967, pp. 407-414.

[20] Wiederhorn, S.M. and Bolz, L.H., "Stress corrosion and static fatigue of glass," *J. Am. Ceram. Soc* **53** [10], 1970, pp. 543-548.

[21] Lawn, B.R., Jakus, K. and Gonzalez, A.C., "Sharp vs blunt crack hypotheses in the strength of glass: a critical study using indentation flaw," *J. Am. Ceram. Soc.* **68** [1], 1985, pp. 25-34.